

Unstable Asia: active deformation of Siberia revealed by drainage shifts

Mark B. Allen¹ and Clare E. Davies^{2,3}

¹Department of Earth Sciences, University of Durham, Durham, DH1 3LE, UK. E-mail: m.b.allen@durham.ac.uk

²CASP, Department of Earth Sciences, University of Cambridge, Cambridge, CB3 0DH, UK

³Woodside Energy Ltd, Perth, Western Australia, Australia

ABSTRACT

Regional incision and lateral shifts of rivers in the West Siberian Basin and surrounding areas show the action of long wavelength surface tilting, directed away from the Urals and Central Asian mountains and towards the Siberian Craton. In the north of the basin, surface uplift of individual folds is recorded by local lateral drainage migration. Lateral slopes of river valleys vary in gradient from 0.001 to 0.0001, generally decreasing with increasing river discharge. As a result of this surface deformation significant drainage shifts are taking place in three of the longest and highest discharge river systems on Earth: the Yenisei, Ob' and Irtysh. The deformation is most plausibly caused by subtle faulting at depth, below the thick basin fill of Mesozoic and Lower Cenozoic sediments. Active deformation of western Siberia appears to represent a previously unrecognised, far-field effect of the India-Eurasia collision, up to ~1500 km north of the limit of major seismicity and mountain building. It adds $\sim 2.5 \times 10^6 \text{ km}^2$ to the region deformed by the collision, which is an area greater than the Himalayas and Tibet combined. It is also an analogue for the formation of low angle unconformities in terrestrial sedimentary basins on the periphery of other orogenic belts.

INTRODUCTION

This paper shows that active deformation occurs within and around the West Siberian Basin (Figs 1 and 2). The west Siberian region is conventionally regarded as part of "stable Asia" in the context of the broad India-Eurasia collision zone, because it lacks significant seismicity and lies below the resolution of earthquake or GPS-derived velocity fields (Avetisov, 1999; Zhang *et al.*, 2004; England & Molnar, 2005; Bayasgalan *et al.*, 2005). We use lateral shifts and anomalies in drainage patterns to reveal the pattern of surface deformation, because they highlight warps and tilts of the landscape in low relief, low strain areas.

The results have a wider implication for continental tectonics, as they demonstrate that long wavelength surface deformation can occur at the periphery of broad collision zones. Such deformation represents a mechanism for generating regional, subtle, angular unconformities in terrestrial sedimentary basins.

The topography and geology of Central and East Asia arise from the continued convergence of the Indian and Eurasian plates since initial collision ~50 million years ago. This process has generated the Himalayas, Tibetan plateau and mountain ranges of Central Asia such as the Tian Shan and Altai (Fig. 1; Molnar & Tapponnier, 1975; Tapponnier *et al.*, 2001). Surface uplift links plausibly to regional and even global climate change (Raymo and Ruddiman, 1992; Molnar *et al.*, 1993; An *et al.*, 2001). Changing topography also re-organizes drainage systems across eastern Eurasia (Clark *et al.*, 2004; Clift & Blusztajn, 2005), such that the late Cenozoic evolution of rivers has provided insights into regional deformation patterns over this period. To date attention

has focused on rivers within high topography, actively deforming areas, or the flexural forelands in front of the Himalayas.

We present a study of the geomorphology of the West Siberian Basin and adjacent areas of Russia (Figs 1-3), and show that long wavelength (100s of km) active surface tilting affects and is revealed by present drainage patterns over the northern half of Eurasia between 60° and 90° E. Local shifts in drainage can be attributed to the growth of individual folds, especially in the north of the basin. Our analysis is intended to highlight the overall picture of active deformation as revealed by the geomorphology. The vast scale of the basin, and the paucity of published work on its neotectonics and geomorphology, makes it a frontier for future research on the interactions of deformation and drainage.

GEOLOGICAL BACKGROUND

The West Siberian Basin has low elevations and relief, predominantly between 0 and 200 m above sea level, and an area of $\sim 3.5 \times 10^6 \text{ km}^2$ including its offshore continuation to the north (Figs 1-3). This is an area on a scale comparable with western Europe. Present drainage in the West Siberian Basin is dominated by three rivers: the Yenisei, Ob' and Irtysh (Fig. 3). The Yenisei hugs the eastern margin of the basin, close to the western edge of the Siberian Craton. The Ob' flows northwest across the southern part of the West Siberian Basin, but passes south of the West Siberian Hills to the point where it is joined by the Irtysh. The combined rivers then flow north. Each of these three rivers is on the scale of the Mississippi in terms of both length and discharge, although their sediment loads are far lower (Milliman & Syvitski, 1992). Their combined drainage basins are $5.6 \times 10^6 \text{ km}^2$ in area. Present discharge from the Ob'/Irtysh and Yenisei is $1024 \text{ km}^3/\text{year}$ in total, and increasing, with implications for Arctic Ocean salinity and thereby the potential to affect North Atlantic Deep Water formation (Peterson *et al.*, 2002). All of the rivers flowing through the West Siberian Basin enter the Arctic Ocean, and erode into Cretaceous – upper Oligocene strata of the basin interior; there are no significant areas within the onshore basin undergoing long-term subsidence and deposition.

Crustal thickness decreases into the basin interior from the margins, from $\sim 50 \text{ km}$ at the western, southern and eastern basin margins to $\sim 36 \text{ km}$ in the southeast of the basin (Vyssotski *et al.*, 2006). It is bordered by the Urals to the west, Siberian Craton to the east, and Central Asian ranges to the south. The basement to the basin is formed by a poorly-known assemblage of buried arcs, accretionary complexes and microcontinents (Bochkarev *et al.*, 2003). These had accreted to each other and the adjacent Siberian and East European cratons by the end of the Paleozoic, during the Altaid orogeny (Şengör & Natal'in, 1996).

The West Siberian Basin originated by rifting near the Permo-Triassic boundary at $\sim 251 \text{ Ma}$, coincident with the Siberian flood basalts (Reichow *et al.*, 2002) and likewise attributed to the impact of a mantle plume. Together, the Permo-Triassic rifts and pre-Late Permian basement faults produce a strong north-south structural grain within the basin and at its eastern and western margins (Şengör and Natal'in 1996; Allen *et al.*, 2006). This is complicated by other trends, including northeast-southwest trending faults – related to oblique rifting, and northwest-southeast trending faults in the south of the basin, related to the Altaid basement grain in this particular area.

Post-rift strata are up to 10 km in thickness. All of the basin stratigraphy is deformed by long wavelength ($\leq 100 \text{ km}$), low amplitude (100s of m) anticlines

(Vyssotski *et al.*, 2006). Individual folds are up to 300 km long (Fig. 3). Folds at least partially correspond to the orientations and locations of pre-Mesozoic basement faults. Many folds lie over or adjacent to basement faults. Folds commonly have a roughly north-south orientation, although there is considerable variation. Folding is conventionally inferred to be Oligocene in age ($> \sim 23$ Ma) and resulting from a brief pulse of deformation, based on the absence of significant post-Oligocene sediments across much of the basin (Kontorovich, 1975; Vyssotski *et al.*, 2006). The exact fold mechanism is enigmatic. There is limited evidence for direct reactivation of basement faults, notwithstanding the coincidence of folds and basement trends, and many folds are located over basement highs, i.e. evidence is lacking for regional inversion of the Permo-Triassic extensional faults. However, on published seismic data and interpretations (Peterson & Clarke, 1991; Vyssotski *et al.*, 2006), the consistent thickness of Mesozoic strata over the basement highs argues against the folds being conventional drape anticlines.

A thin covering (typically 10s m) of Quaternary fluvio-glacial and loess sediments (Arkhipov *et al.*, 1997) is present in the southeast of the basin. Elsewhere Tertiary or Cretaceous strata are the exposed bedrock, albeit typically covered by extensive peat deposits and vegetation.

METHODS

We used Landsat and Aster satellite imagery and digital elevation models for analysis of the geomorphology of the study area. The latter datasets are based on GTOPO30 and SRTM data. SRTM data are only available for south of 60° N. The pixel size of the GTOPO30 data is ~ 1 km, compared with ~ 90 m for SRTM, but the scale of the drainage systems is such that the coarser resolution is adequate for determining first order patterns in the geomorphology. MrSID format mosaics of Landsat 7 satellite imagery (bands 2, 4, 7) were used for larger areas. Standard procedures in ArcGIS were used for combining and analysing all datasets.

In the low gradient river systems of the West Siberian Basin (Table 1), systematic lateral drainage migrations are very useful for detecting areas of local surface uplift and tilting produced by active folding. Therefore a key aspect of this study is mapping the regional pattern of such migrations. One or more of the following criteria for surface tilting were used to interpret an external forcing for lateral migration: asymmetric incision profiles, unpaired terraces (that is, terraces on only one side of the river valley, caused by active tilting transverse to an incising river), asymmetric drainage basins, preferential orientation of meander scars (Leeder & Alexander, 1987; Marple & Talwani, 2000; Cox *et al.*, 2001).

Additional criteria for active fold and drainage interactions are subtle variations in the planform of rivers as they cross zones of active uplift or subsidence (Burbank *et al.*, 1996a; Holbrook & Schumm, 1999), with changes between meandering, anastomosing and braided forms, and/or changes in sinuosity (defined as river length divided by valley length; Holbrook & Schumm, 1999; Ouchi, 1985). These latter criteria are less obvious in the rivers of the West Siberian Basin, perhaps because gradients are so low: the Ob' is at an elevation of only ~ 70 m above sea-level at Novosibirsk, ~ 2200 km from its estuary, equivalent to a gradient of 0.000035.

OBSERVATIONS

Individual fold and drainage interactions

Fold and drainage interactions are most obvious in the zone south of the Pleistocene ice sheet limit ($\sim 67\text{-}68^\circ \text{N}$) and north of the drainage divide of the West Siberian Hills. North of the ice sheet limit the geomorphology is affected by glacial or peri-glacial features and also undergoes isostatic rebound following glacial loading and subsequent melting (Mangerud *et al.*, 2002; Mangerud *et al.*, 2004; Peltier, 2004; Svendsen *et al.*, 2004). This glacial influence may be why exposure levels are generally deeper in the north of the basin (Nalivkin, 1983), despite this area having the thickest Mesozoic-Cenozoic stratigraphy.

Several major fold axes north of 65°N coincide with local drainage divides (Fig. 3), including the Urengoy anticline (including the supergiant Yamburg gas field), and the Yarudey and Chasel anticlines (Vyssotski *et al.*, 2006). The northern reaches of the Pur and Taz rivers lie in the synclines between the Urengoy and Chasel anticlines and the Yenisei monocline (Fig. 3). There is some evidence of lateral channel migration on the limbs of these anticlines, although this is limited, perhaps because the main south-north rivers are roughly equidistant from the fold axes. For example, the lowermost 50 km of the Pur river hugs the east side of the 25 km wide floodplain, eroding into 50 m high cliffs.

Further examples of drainage migration or structural control of drainage are shown in Figs. 4-7. At the northwest margin of the basin the Ob' changes course to flow eastwards along the southern limb of an east-west anticline at the eastern margin of the Urals. This anticlinal uplift is known as the Schchuchya zone (Fig. 4; Puchkov, 1997), and lies at the junction of the northern ("Polar") Urals and the northwest-southeast trending Pay-Khoy zone, which in turn links the Urals to Novaya Zemlya. To the north of the Schchuchya zone, Baydaratskaya Bay is on the scale and proportions of the present estuary of the Ob', but the Baydarata river flowing into the head of the bay has a drainage basin on the order of $10,000 \text{ km}^2$ (Fig. 4). This is completely out of proportion with the scale of the bay. The lowest elevation on the present drainage divide between the Ob' estuary and Baydaratskaya Bay is at $\sim 50 \text{ m}$ above sea-level. Drainage patterns are locally highly convoluted in this region: one river changes direction through 180° degrees, first flowing northwards, then east, then south to join the Ob' near its estuary. We speculate that Baydaratskaya Bay was the estuary for the Ob' before drainage was deflected to the east by tectonically-driven surface uplift of the Schchuchya zone. However, the Schchuchya zone is also the southern limit of Early Weichselian ($\sim 90 - 80 \text{ ka}$) ice sheets (Svendsen *et al.*, 2004), which provide an alternative mechanism for re-routing the Ob'. The two mechanisms are not mutually exclusive.

The Lyamin Arch (anticline) in the northwest of the basin causes local surface tilt, and drainage migration of the Nazym river to the west (Fig. 5). This river has a markedly asymmetric drainage basin, with eastern (left bank) tributaries up to 20 times longer than their western counterparts. Meander scars are preferentially located east of the present course of the Nazym, and are preferentially oriented in a concave direction towards the main channel, indicating gradual tilting and channel migration across the floodplain towards the west (Leeder & Alexander, 1987). They are also on much larger scales than the present meander loops (2-3 times the diameter; Fig. 6), indicating higher discharge rates in the past. We have no constraints on how long ago these meander scars were formed. Lateral gradient across the Nazym valley is ~ 0.001 . At the same latitude as the Nazym, the Ob' appears to be migrating to the east: the present river

channel is located at the eastern side of the floodplain, with an unpaired terrace to its west, some 50 m above sea-level. Thus a narrow neck of land, 30 km across with maximum relief of ~125 m above the adjacent floodplains, is being eroded from both its western and eastern flanks (Fig. 5).

The Taz river also shows examples where active uplift is affecting the river planform (Fig. 7). Meander scars are preferentially oriented in a concave direction towards the main channel, indicating gradual tilting and channel migration across the floodplain towards the north and northeast in this region. Lateral gradient across the valley is ~0.001. The uplifted region west of the river corresponds to the southern part of the Chasal anticline (Vyssotski *et al.*, 2006), such that surface uplift associated with the fold appears to be responsible for the lateral drainage migration.

Rivers flowing down the flanks of the West Siberian Hills (Fig. 3) show little evidence for systematic lateral drainage migration, but moderate (10-20 m) incision along braided reaches. This area is underlain by extensive and adjacent sub-surface folds, principally the Surgut and Nizhnevartovsk arches, which are not individually discernible in the geomorphology.

Overall, the presence and pattern of surface deformation in the north of the West Siberian Basin (north of ~61° N) is consistent with major folds in this region being active structures, controlling the observed drainage patterns.

Regional drainage patterns: overview

Maximum incision of low relief landscapes at the basin margins varies from ~200 m in the southeast to ~80 m at the western margin. Incision decreases towards the basin interior, reduced to <20 m by the east-west reach of the Ob' at ~61° N. The important point is that all areas of the basin are undergoing surface uplift and tilting on at least some scale, even though as a whole the landscape is one of the largest sub-aerial low relief areas on Earth.

Using the same criteria for surface tilting as used to pick out active individual folds, it is possible to detect regional lateral migration and tilt patterns in the southern part of the basin, particularly between the upper reaches of the Ob' and the Irtysh rivers. Unlike further north, it is difficult to attribute these lateral migrations and tilts to individual structures.

The regional lateral migration pattern for the basin and adjacent areas is shown on Fig. 8. Individual arrows represent lateral migration azimuths identified from analysis of the satellite images and the DEMs; each arrow summarises a 10,000 km² area. Adjacent areas have ~50% overlap. Lateral migration on an individual reach does not necessarily represent the true local tilt direction, but the variable orientation of reaches in trellis and dendritic drainages allows regional tilt azimuths to be mapped in a semi-quantitative manner. The results show west to east tilting across the whole West Siberian Basin south of ~61° N, combined with northwards tilt away from the Central Asian ranges. No regional tilt is identifiable north of ~61° N in the basin interior, where individual folds determine surface deformation patterns as described above. Eastward tilting occurs ≤200 km east of the Urals and ≤100 km west of the Siberian Craton, for long distances parallel to these basin margins, particularly in the main south-north flowing rivers (the Tobol-Irtysh-Ob' system is parallel to the Urals and the Yenisei is parallel and adjacent to the Siberian Craton). West to east tilt across the east of the basin interior is against regional topographic and crustal thickness gradients (Vyssotski *et al.*, 2006), and commonly in a different direction to local bedrock dip.

Ob', Irtysh and Tobol

On the scale of the largest rivers, the combined Ob', Irtysh and Tobol system in the western part of the basin has active channels at the northern limits of the floodplain in east-west reaches, or at the eastern limit of north-south reaches (Figs. 3 and 8). Unpaired terraces are preserved on the southern and western sides of these channels, respectively. Tributaries typically possess asymmetric topographic cross-sections, indicating tilt to the east (north-south reaches) or north (east-west reaches). Lateral gradients are typically 0.0001 – 0.0005 across the floodplains. These relationships occur for >1500 km, from southern reaches of the Irtysh within the basin to near the estuary of the Ob' in the Arctic Ocean.

Both the Irtysh and the Ob' take large convex-northeast loops from close to their entry points into the basin, changing to south-to-north courses once they have joined the Tobol and each other (Fig. 3). Similar-shaped loops are present in smaller rivers to the east as far as 97° E. Such patterns may reflect originally straighter courses, deflected by tilting to the east or northeast. Longitudinal river profiles do not show perturbations, presumably because low river gradients, long length scales and low tilt rates do not produce clear knickpoints.

Lateral migration also occurs in numerous smaller rivers, revealed by asymmetric valley profiles. Examples include the left-bank tributaries of the Ob' in the region of 80° E (Fig. 9), where asymmetric valley profiles in a very low relief landscape suggest lateral migration to the ESE. Lateral river valley gradients are ~0.001. Bedrock in this region is Oligocene in age, with a thin cap of Quaternary in the south. Fold axes in this area trend northwest-southeast (Fig. 3); it is therefore implausible that lateral drainage migration is controlled by bedrock dip on the limbs of these local folds.

Other prominent examples of lateral migration are river valleys between the Ob' and the Yenisei in the southeast of the basin, in the vicinity of the Chulym river and its tributaries (Fig. 3). These valleys consistently have asymmetric cross-section profiles, such that the regional surface tilt appears to be to the east or ENE. This observation is unexpected, given that this area lies adjacent to bedrock exposures at the northern side of the Altai mountains: if any regional tilt was expected, it would be directed towards or away from the mountain front.

The southern margin of the basin on Russian structural maps is highlighted as the Altay-Sayan monocline (Surkov & Zhero, 1981; Fig. 3). The Ob', Irtysh and their tributaries in this region show characteristic changes in river planform, from straight, confined channels to meandering reaches. Similar trends are repeated in many of the smaller tributaries of the Ob'. These rather abrupt changes in planform may indicate the influence of the edge of this warped basin margin on the drainage systems.

Unpaired terraces are present at various scales throughout the west Siberian landscape, and typically found where there are asymmetric valley profiles. Laterally persistent examples occur south of the Irtysh, where three unpaired terraces are present (Fig. 10). The terrace scarps lie roughly 70, 130 and 200 km south of the Irtysh and east of its confluence with the Tobol, at the southern sides of terraces at ~60, ~80, and ~125 m above sea level respectively. The lower two terraces may correlate with regional terraces identified as the products of late Pleistocene ice-dammed lakes, dated at ~23-12 ka and ~110-75 ka (Arkhipov, 1998).

Smaller scale features are visible south of east-west reaches of the Tom' River, in the southeast of the basin, such as the unpaired terrace at ~235 m above sea-level, picked out in SRTM data in Fig. 11. North-south topographic profiles through this area show up the alluvial terrace ~3 km south of the modern river channel, with an edge ~12 m high. The terrace faces 100 m high cliffs on the north bank of the same reach (Fig. 12); the valley topographic profile is markedly asymmetric. On the south side of the river alluvial deposits of the terrace blanket the tributary valleys of the Tom'. These deposits are only incised at the northern ends of these tributaries, close to the terrace edge and the modern floodplain. Surface tilt indicators are both to the east and north in this area: asymmetric valley profiles south of the Tom' indicate a component of west-to-east tilt (Fig. 11). Numerous local streams to the south and southeast of the basin are flanked by unpaired alluvial terraces below the spatial resolution of SRTM data (Fig. 13). Several rivers in this area are joined by tributaries with obtuse angles upstream of the confluences, consistent with the capture of south-flowing streams by drainage flowing north towards the Ob' or Yenisei.

Yenisei

The Yenisei river enters the West Siberian Basin in the southeast, and follows the eastern margin of the basin, i.e. the western edge of the Siberian Craton, northwards towards the Arctic (Fig. 3). Some authors place the basin margin 150 km west of the present course of the Yenisei, at the western limit of a structural zone known as the Yenisei Monocline (e.g. Vyssotski *et al.*, 2006), but this zone is where the Mesozoic and Lower Tertiary basin fill is tilted towards the west, i.e. the basin interior, rather than the true boundary between the basin and the Siberian craton. Within the Yenisei river valley the active channel lies consistently towards the eastern margin for two 500 km long reaches north and south of ~62° N (Figs. 3 and 8). Unpaired terraces lie on the left bank (west). Late Pleistocene proglacial terraces have been reported in this area (Arkhipov, 1998), but there are no firm regional constraints on terrace age or origin. Lateral gradients across the Yenisei river valley are ~0.0002 – 0.0004. Therefore the regional geomorphology of the river valley suggests active tilting of the landscape towards the east. At ~62° N there is an isolated uplift near the basin margin, which constrains the Yenisei to a narrower floodplain. This localised uplift represents the eastern limit of the West Siberian Hills; no individual structural feature is marked in this area on the basin-wide maps of Surkov & Zhero (1981) or Vyssotski *et al.* (2006).

Rates of deformation

Some estimates are possible for the rate of both individual fold growth and regional rock uplift and tilting. Fold growth has occurred since the last regional deposition (latest Oligocene, ~25 Ma), implying that rock uplift rates on anticline crests are in the order of 0.01 mm/year. It is not clear whether deformation has been continuous or episodic over this time, and deformation could have begun more recently, making this estimate a lower bound. A first order estimate of the regional west-to-east tilt rate in the south of the West Siberian Basin can be derived from the warp of the top of the youngest, late Eocene, marine strata in the basin: this is ~400 m over ~1000 km from the eastern side of the Urals to the southeast of the basin (Fig. 14), derived from Vyssotski *et al.* (2006) and geological map data (Nalivkin, 1983). This corresponds to a maximum rate of ~0.02 mm/year, if deformation began at ~25 Ma. Again, it is possible that deformation began more recently. It represents a lateral gradient of 0.0004, similar

to the present day lateral valley gradients in the south-to-north reaches of the Irtysh and Ob'. Both uplift estimates are very approximate, but emphasise that rates of rock uplift are at least two orders of magnitude slower than within the Himalayas (Burbank *et al.*, 1996b). Strain rates are obviously extremely low, and the overall contribution to the India-Eurasia convergence is insignificant.

Lateral valley gradients of the largest rivers in the basin (Yenisei, Ob' and Irtysh) are 0.0001 – 0.0005, where tectonic tilt is inferred (Table 1). Gradients are higher for smaller river valleys such as the Taz and Nazym: ~0.001. If the modern river valleys initiated during the major deglaciation of the Fennoscandian ice sheet at ~15 ka BP, these gradients are equivalent to tilt rates of $7 \times 10^{-6} - 3 \times 10^{-5}$ radians kyr⁻¹ for the largest rivers and 7×10^{-5} radians kyr⁻¹ for their main tributaries. All of these values are slow compared with tilt rates calculated for the floodplains of tectonically active half grabens (roughly 10^{-4} radians kyr⁻¹; Peakall *et al.*, 2000). Consistent with these low rates, the river response to lateral tilting in the West Siberian Basin is gradual migration rather than abrupt avulsion.

DISCUSSION

Cenozoic folding in the West Siberian Basin has been attributed to a far-field effect of the India-Asia collision (e.g. Vyssotski *et al.*, 2006). No other cause seems viable. Arctic tectonics are dominated by the very slow and intermittent spreading of Gakkel (Arctic) mid-ocean ridge (e.g. Sekretov, 2002; Dick *et al.*, 2003), which is a less plausible mechanism for generating strain far into the continental interior. The geomorphology in the northern part of the basin indicates that deformation is active ~1500 km north of the present limit of major seismicity within western Mongolia and the Altai mountains (Bayasgalan *et al.* 2005), and ~3500 km north of the original India-Eurasia suture. Fold axis orientations are commonly at a low angle to the roughly-north-south India-Eurasia convergence vector, which would not be expected if the Siberian crust was isotropic. The structural grain of the basement (Allen *et al.*, 2006) appears to exert a strong control on Cenozoic fold location and orientation.

Incision and tilting at the southern and western sides of the West Siberian Basin is a regional effect that decays in amplitude into the basin interior, but is still discernible >1000 km from the basin margins (Fig. 8). The change between regional surface tilt and localised lateral drainage migration occurs at about 61° N, at the latitude of the West Siberian Hills, but it is unclear why.

Regional west-to-east tilt in the west of the West Siberian Basin is in the same direction as the regional bedrock dip (Figs 2 and 8). East of ~65° E this is not the case: lateral migration and surface tilt are commonly in the opposite direction to the bedrock dip. Thus the overall drainage migration patterns are not merely passive responses to pre-existing bedrock configurations. Even in the west of the basin we argue that the combination of active incision and lateral migration makes it unlikely that rivers are simply controlled by bedrock dip in a tectonically-inactive setting.

Variable, but low degrees of crustal thickening and isostatic uplift at the range margins and within the basin is the likely cause of the regional surface uplift and tilt patterns. Sub-surface data support this, showing all post-Triassic strata dipping east of the Urals and north of the Central Asian mountains respectively (Fig. 14). This deformation presumably takes place by discrete faults and folds at depth, similar to the examples beginning to be published on seismic datasets (Vyssotski *et al.*, 2006), with

displacements merging and dying out upwards to produce the smooth regional tilts observed at the surface.

Other possible surface uplift mechanisms are less plausible. The surface tilt is not the result of deglaciation within the study area itself: there are no documented Pleistocene ice sheets within the interior of the West Siberian Basin, the Urals, or Central Asia to the south. Far-field isostatic effects caused by the Scandinavian or Laurentian ice sheets are plausible within the Eurasian continental interior, but initial modelling indicates that such effects are much smaller than the observed rock uplift and have the wrong spatial distribution (Whitehouse *et al.*, in press). The monotonic nature of the tilting argues against lithospheric scale buckle folding of the kind suggested by Cloetingh *et al.* (1999) for several areas of Eurasia. Lower crustal flow away from thickened crust is a mechanism for producing isostatic uplift (Royden *et al.*, 1997), but in the east of the basin tilt directions are towards thicker crust, i.e. exactly the opposite to what would be expected if such a mechanism was operating. The length scales of the Siberian deformation and surface tilting are too long for erosional unloading of a foreland adjacent to a mountain belt (Burbank, 1992), especially as there is nothing unusual about the strength of the west Siberian lithosphere (effective elastic thickness ≤ 25 km, McKenzie & Fairhead, 1997).

The geometry of the Yenisei River at the eastern margin of the basin resembles the axial drainage of flexural, foreland basins, lying parallel and close to a topographic front. It is clear that there has been Cenozoic deformation along the western side of the Siberian Craton: Upper Cretaceous and lower Tertiary strata are gently folded and tilted to the west in the Yenisei Monocline. Starosel'tsev *et al.* (2003) show an upper crustal-scale, east-dipping blind thrust at the western side of the craton, which terminates to the west in Palaeozoic strata beneath the Mesozoic sediments of the West Siberian Basin. However, there is only minor historical seismicity in the region, and no evidence for a thick, late Cenozoic, sedimentary wedge at the basin margin. A flexural control on the position of the Yenisei adjacent to the craton is therefore possible, but not proven, and more work on the structure of this area is needed. Whatever the underlying mechanism, the surface tilting towards the Siberian Craton is opposite in sense to the tilting away from the Urals and the Central Asian ranges (in that it is towards the basin margin, not away from it), and directly opposite to the westwards tilt of Cretaceous/Paleogene strata adjacent to the craton margin (Figs 2 and 8).

SUMMARY

Our results show that there is subtle, active surface deformation of western Siberia, involving both long wavelength tilting of the landscape and drainage perturbations over individual folds (Fig. 8). Three of the largest rivers in the world - the Yenisei, Ob' and Irtysh - are actively changing course as the result of this deformation. These effects are consistent with the action of a low degree of crustal thickening at the periphery of the India-Eurasia collision, and reveal broadly distributed, effectively continuum deformation far below the present resolution of GPS-derived velocity fields.

While the proportion of the overall plate convergence is insignificant, the area affected in Siberia - $\sim 2.5 \times 10^6$ km² - is larger than the Himalayas and Tibet combined (Fig. 1), and uplift has interrupted a 200 million year history of deposition in one of the largest continental basins on Earth. Thus as well as greatly expanding the known deformation field of the India-Eurasia collision, the west Siberian surface deformation provides a possible analogue for low angle, regional unconformities developed in

continental interiors throughout the geological record (e.g. Mitrovica *et al.*, 1996; Boote *et al.*, 1998; Scott *et al.*, 2000). In some places such unconformities have been attributed to mantle effects, such as dynamic topography generated above an active subduction zone. The active west Siberian case shows that a much more prosaic mechanism is also plausible, related to the cumulative activity of low amplitude, long wavelength folds in the basin fill, themselves generated above subtle basement faults.

Acknowledgements

We thank the sponsors of the CASP West Siberian Basin Project, where part of this work originated. Jamie Stewart and Stewart Sinclair provided GIS support. Stuart Jones, Chris Saville and Richard Davies made useful comments during the writing of the paper. We thank Peter Clift and two anonymous referees for useful reviews. Field photographs were taken during collaborative work with the Siberian Branch, Russian Academy of Sciences on the Mesozoic evolution of southern Siberia: we acknowledge Misha Buslov and Inna Safonova.

References

- ALLEN, M.B., ANDERSON, L., SEARLE, R.C. & BUSLOV, M.M. (2006) Oblique rift geometry of the West Siberian Basin: tectonic setting for the Siberian flood basalts. *Journal of the Geological Society*, **163**, 901-904.
- AN, Z., KUTZBACH, J.E., PRELL, W.L. & PORTER, S.C. (2001) Evolution of Asian monsoons and phased uplift of the Himalayan Tibetan plateau since Late Miocene times. *Nature*, **411**, 62-66.
- ARKHIPOV, S.A., ZYKINA, V.S., KRUKOVER, A.A. & GNIBIDENKO, Z.N. (1997) Stratigraphy and paleomagnetism of glacial and loess-soil deposits on the West-Siberian Plain. *Russian Geology and Geophysics*, **38**, 1027-1048.
- ARKHIPOV, S.A. (1998) Stratigraphy and paleogeography of the Sartan glaciation in West Siberia. *Quaternary International*, **45-46**, 29-42.
- AVETISOV, G.P. (1999) Geodynamics of the zone of continental continuation of Mid-Arctic earthquakes belt (Laptev Sea). *Physics of the Earth and Planetary Interiors*, **114**, 59-70.
- BAYASGALAN, A., JACKSON, J. & MCKENZIE, D. (2005) Lithosphere rheology and active tectonics in Mongolia: relations between earthquake source parameters, gravity and GPS measurements. *Geophysical Journal International*, **163**, 1151-1179.
- BOCHKAREV, V.S., BREKHUNTSOV, A.M. & DESHCHENYA, N.P. (2003) The Paleozoic and Triassic evolution of West Siberia. *Russian Geology and Geophysics*, **44**, 120-143.
- BOOTE, D.R.D., CLARK-LOWES, D.D. & TRAUT, M.W. (1998) Palaeozoic Petroleum Systems of North Africa. In: *Petroleum Geology of North Africa* (Ed. by D. C. McGregor, R. T. J. Moody & D. D. Clark-Lowes), **132**, 7-68. Special Publication of the Geological Society of London.
- BURBANK, D., MEIGS, A. & BROZOVIC, N. (1996a) Interactions of growing folds and coeval depositional systems. *Basin Research*, **8**, 199-223.
- BURBANK, D.W. (1992) Causes of recent Himalayan uplift deduced from deposited patterns in the Ganges basin. *Nature*, **357**, 680-683.

- BURBANK, D.W., LELAND, J., FIELDING, E., ANDERSON, R.S., BROZOVIC, N., REID, M.R. & DUNCAN, C. (1996b) Bedrock incision, rock uplift and threshold hillslopes in the northwestern Himalayas. *Nature*, **379**, 505-510.
- CLARK, M.K., SCHOENBOHM, L.M., ROYDEN, L.H., WHIPPLE, K.X., BURCHFIEL, B.C., ZHANG, X., TANG, W., WANG, E. & CHEN, L. (2004) Surface uplift, tectonics, and erosion of eastern Tibet from large-scale drainage patterns. *Tectonics*, **23**, 10.1029/2002TC001402.
- CLIFT, P.D. & BLUSZTAJN, J. (2005) Reorganization of the western Himalayan river system after five million years ago. *Nature*, **438**, 1001-1003.
- CLOETINGH, S., BUROV, E. & POLIAKOV, A. (1999) Lithosphere folding: primary response to compression? (from Central Asia to Paris Basin). *Tectonics*, **18**, 1064-1083.
- COX, R.T., VAN ARSDALE, R.B. & HARRIS, J.B. (2001) Identification of possible Quaternary deformation in the northeastern Mississippi embayment using quantitative geomorphic analysis of drainage-basin asymmetry. *Geological Society of America Bulletin*, **113**, 615-624.
- DICK, H.J.B., LIN, J. & SCHOUTEN, H. (2003) An ultraslow-spreading class of ocean ridge. *Nature*, **426**, 405-412.
- ENGLAND, P. & MOLNAR, P. (2005) Late Quaternary to decadal velocity fields in Asia. *Journal Of Geophysical Research-Solid Earth*, **110**, 10.1029/2004JB003541.
- HOLBROOK, J. & SCHUMM, S.A. (1999) Geomorphic and sedimentary response of rivers to tectonic deformation: a brief review and critique of a tool for recognizing subtle epeirogenic deformation in modern and ancient settings. *Tectonophysics*, **305**, 287-306.
- KONTOROVICH, A.E. (1975) *Geology of Oil and Gas of West Siberia*. Nedra, Moscow.
- LEEDER, M.R. & ALEXANDER, J. (1987) The origin and tectonic significance of asymmetrical meander-belts. *Sedimentology*, **34**, 217-226.
- MANGERUD, J., ASTAKHOV, V. & SVENDSEN, J.I. (2002) The extent of the Barents-Kara ice sheet during the last glacial maximum. *Quaternary Science Reviews*, **21**, 111-119.
- MANGERUD, J., JAKOBSSON, M., ALEXANDERSON, H., ASTAKHOV, V., CLARKE, G.K.C., HENRIKSEN, M., HJORT, C., KRINNER, G., LUNKKA, J.P., MOLLER, P., MURRAY, A., NIKOLSKAYA, O., SAARNISTO, M. & SVENDSEN, J.I. (2004) Ice-dammed lakes and rerouting of the drainage of northern Eurasia during the last glaciation. *Quaternary Science Reviews*, **23**, 1313-1332.
- MARPLE, R.T. & TALWANI, P. (2000) Evidence for a buried fault system in the coastal plain of the Carolinas and Virginia - implications for neotectonics in the southeastern United States. *Geological Society of America Bulletin*, **112**, 200-220.
- MCKENZIE, D. & FAIRHEAD, D. (1997) Estimates of the effective elastic thickness of the continental lithosphere from Bouguer and free air gravity anomalies. *Journal of Geophysical Research*, **102**, 27523-27552.
- MILLIMAN, J.D. & SYVITSKI, J.P.M. (1992) Geomorphic tectonic control of sediment discharge to the ocean - the importance of small mountainous rivers. *Journal of Geology*, **100**, 525-544.
- MINISTRY OF GEOLOGY OF THE USSR (1965) Geological map of the USSR, 1:2,500,000.
- MITROVICA, J.X., PYSKLYWEC, R.N., BEAUMONT, C. & RUTTY, A. (1996) The Devonian to Permian sedimentation of the Russian platform: an example of subduction-

- controlled long-wavelength tilting of continents. *Journal of Geodynamics*, **22**, 79-96.
- MOLNAR, P. & TAPPONNIER, P. (1975) Cenozoic tectonics of Asia: effects of a continental collision. *Science*, **189**, 419-426.
- MOLNAR, P., ENGLAND, P. & MARTINOD, J. (1993) Mantle dynamics, uplift of the Tibetan plateau and the Indian monsoon. *Reviews of Geophysics*, **31**, 357-396.
- NALIVKIN, D.V. (1983) Geological map of the USSR and adjacent water-covered areas, Ministry of Geology of the USSR. Moscow.
- OUCHI, S. (1985) Response of alluvial rivers to slow active tectonic movement. *Bulletin of the Geological Society of America*, **96**, 504-515.
- PEAKALL, J., LEEDER, M., BEST, J. & ASHWORTH, P. (2000) River Response to Lateral Ground Tilting: A Synthesis and Some Implications for the Modelling of Alluvial Architecture in Extensional Basins. *Basin Research*, **12**, 413-424.
- PELTIER, W.R. (2004) Global glacial isostasy and the surface of the ice-age Earth: the ICE-5G (Vm2) model and GRACE. *Annual Review of Earth and Planetary Sciences*, **32**, 111-149.
- PETERSON, B.J., HOLMES, R.M., MCCLELLAND, J.W., VOROSMARTY, C.J., LAMMERS, R.B., SHIKLOMANOV, A.I., SHIKLOMANOV, I.A. & RAHMSTORF, S. (2002) Increasing river discharge to the Arctic Ocean. *Science*, **298**, 2171-2173.
- PETERSON, J. A. & CLARKE, J. W. (1991) *Geology and hydrocarbon habitat of the West Siberian Basin*. AAPG Studies in Geology **32**.
- PUCHKOV, V.N. (1997) Structure and geodynamics of the Uralian orogen. In: *Orogeny through Time* (Ed. by J.-P. Burg & M. Ford), **121**, 201-236. Geological Society Special Publication.
- RAYMO, M.E. & RUDDIMAN, W.F. (1992) Tectonic forcing of Late Cenozoic climate. *Nature*, **359**, 117-122.
- REICHOW, M.K., SAUNDERS, A.D., WHITE, R.V., PRINGLE, M.S., AL'MUKHAMEDOV, A.I., MEDVEDEV, A.I. & KIRDA, N.P. (2002) Ar-40/Ar-39 Dates from the West Siberian Basin: Siberian flood basalt province doubled. *Science*, **296**, 1846-1849.
- ROYDEN, L.H., BURCHFIEL, B.C., KING, R.W., WANG, E., CHEN, Z.L., SHEN, F. & LIU, Y.P. (1997) Surface deformation and lower crustal flow in eastern Tibet. *Science*, **276**, 788-790.
- SCOTT, D.L., RAWLINGS, D.J., PAGE, R.W., TARLOWSKI, C.Z., IDNURM, M., JACKSON, M.J. & SOUTHGATE, P.N. (2000) Basement framework and geodynamic evolution of the Palaeoproterozoic superbasins of north-central Australia: an integrated review of geochemical, geochronological and geophysical data. *Australian Journal of Earth Sciences*, **47**, 341-380.
- SEKRETOV, S.B. (2002) Structure and tectonic evolution of the southern Eurasia Basin, Arctic Ocean. *Tectonophysics*, **351**, 193-243.
- ŞENGÖR, A.M.C. & NATAL'IN, B.A. (1996) Paleotectonics of Asia: fragments of a synthesis. In: *The Tectonic Evolution of Asia* (Ed. by A. Yin & M. Harrison), 486-640. Cambridge University Press, Cambridge.
- STAROSEL'TSEV, V.S., MIGURSKII, A.V. & STAROSEL'TSEV, K.V. (2003) The Yenisei Range and its junction with the Siberian platform and West Siberian plate. *Russian Geology and Geophysics*, **44**, 76-85.
- SVENDSEN, J. I., ALEXANDERSON, H., ASTAKHOV, V. I., DEMIDOV, I., DOWDESWELL, J. A., FUNDER, S., GATAULLIN, V., HENRIKSEN, M., HJORT, C., HOUMARK-NIELSEN,

- M., HUBBERTEN, H. W., INGOLFSSON, O., JAKOBSSON, M., KJAER, K. H., LARSEN, E., LOKRANTZ, H., LUNKKA, J. P., LYSÄ, A., MANGERUD, J., MATIOUCHKOV, A., MURRAY, A., MOLLER, P., NIESSEN, F., NIKOLSKAYA, O., POLYAK, L., SAARNISTO, M., SIEGERT, C., SIEGERT, M. J., SPIELHAGEN, R. F. & STEIN, R. (2004) Late Quaternary ice sheet history of northern Eurasia. *Quaternary Science Reviews*, **23**, 1229-1271.
- SURKOV, V.S. & ZHERO, O.G. (1981) *Basement and Development of the Platform Cover of the West Siberian Platform*. Nedra, Moscow.
- TAPPONNIER, P., XU, Z.Q., ROGER, F., MEYER, B., ARNAUD, N., WITTLINGER, G. & YANG, J.S. (2001) Oblique Stepwise Rise and Growth of the Tibet Plateau. *Science*, **294**, 1671-1677.
- VYSSOTSKI, A.V., VYSSOTSKI, V.N. & NEZH DANOV, A.A. (2006) Evolution of the West Siberian Basin. *Marine and Petroleum Geology*, **23**, 93-126.
- WHITEHOUSE, P.L., ALLEN, M.B. & MILNE, G.A. (in press) Glacial isostatic adjustment as a control on coastal processes: An example from the Siberian Arctic. *Geology*.
- ZHANG, P.-Z., SHEN, Z., WANG, M., GAN, W., BÜRGMANN, R., MOLNAR, P., WANG, Q., NIU, Z., SUN, J., WU, J., SUN, H. & YOU, X. (2004) Continuous deformation of the Tibetan plateau from global positioning system data. *Geology*, **32**, 809-812.

Figure captions

- Fig. 1.** Location of the West Siberian Basin and the topography of central and eastern Asia, derived from GTOPO30 data.
- Fig. 2.** Geological map of the West Siberian Basin, highlighting the distribution of Cretaceous-Cenozoic strata. From Ministry of Geology of the USSR (1965).
- Fig. 3.** Simplified geography and structure of the West Siberian Basin and surrounding areas. Major anticline axes from Vyssotski *et al.* (2006): Ch, Chasel; Ly, Lyamin; Ni, Nizhnevartovsk; Schchuchya; Su, Surgut; Ur, Urengoy; Ya, Yarudey. The dashed line corresponds to the boundary of the West Siberian Basin. X-Y indicates the location of the regional seismic profile sketched in Fig. 14. Topography derived from GTOPO30 data.
- Fig. 4.** Landsat 7 (MrSID) satellite mosaic of the present Ob' estuary and adjacent areas (bands 2,4,7). The Baydarata river has misfit drainage on the scale of Baydaratskaya Bay. Location shown on Fig. 2.
- Fig. 5.** GTOPO30 topography of the Nazym river and its confluence with the Ob'. Lateral drainage migration of the Nazym appears to be a consequence of surface uplift and tilting of the Lyamin Arch. Dashed line shows Nazym river meander scars. Location shown on Fig. 2.
- Fig. 6.** Landsat 7 (MrSID) image of meander scars, east of the Nazym river, showing the different size of present and past meander loops (bands 2,4,7). Location shown on Fig. 5.
- Fig. 7.** Landsat 7 (MrSID) image of part of the Taz river, showing meander scars preferentially developed to the west of the present river, indicating lateral drainage migration to the northeast and north (bands 2,4,7). Location shown on Fig. 2.
- Fig. 8.** Summary lateral drainage migration in the West Siberian Basin. (A) Arrows give lateral channel migration directions based on geomorphic criteria

within 10,000 km² bins, visible on satellite and/or DEM data and based on criteria discussed in the text. (B) Summary of tilt pattern in (A).

Fig. 9. Examples of active lateral drainage migration: SRTM topography of tributaries on the left (south) bank of the Ob' at ~57° N 80° E in map view and cross-section, showing lateral channel migration to the ESE. This is against regional topographic and crustal thickness gradients. Location shown on Fig. 2.

Fig. 10. Unpaired terraces on the south side of the Irtysh, picked out in SRTM topography. Dashed lines mark terrace edges. These terraces may relate to Pleistocene ice-dammed lakes (Arkhipov, 1998). See text for discussion. Location shown on Fig. 2.

Fig. 11. SRTM topography of an east-west reach of the Tom' river in the range 200-300 m, draped over a Landsat 7 image (bands 2,4,7). An unpaired terrace lies on the south bank at altitude ~235 m; the terrace edge is marked by the dashed line. Location shown on Fig. 2.

Fig. 12. View to the west of a ~100 m high cliff on the north bank of the Tom' river at 53° 47' 40" N 87° 37' 45" E. The location of this cliff is shown on Fig. 11.

Fig. 13. View to the east of a minor unpaired terrace (arrowed), to the south of the West Siberian Basin (location: 53° 03' 12" N 85° 39' 46" E). The terrace height is ~5 m.

Fig. 14. Cross-section through the southern West Siberian Basin (simplified from Vyssotski *et al.*, 2006). Location shown on Figs. 2 and 3. Mesozoic and Tertiary strata dip east from the eastern margin of the Urals. The approximate top of the youngest (Upper Eocene) marine strata is shown to indicate the late Cenozoic bedrock tilt.

Table 1. River valley gradients.

| River system | Gradient |
|--|------------------|
| Overall longitudinal gradient, Ob' | 0.000035 |
| Lateral valley gradient, middle reaches of the Yenisei | ~0.0002 – 0.0004 |
| Lateral valley gradient, western area tributaries of the Ob', Irtys, Tobol | ~0.0001 – 0.0005 |
| Lateral valley gradient, SE area tributaries of the Ob' | ~0.001 |
| Lateral valley gradient, Nazym | ~0.001 |
| Lateral valley gradient, Taz | ~0.001 |

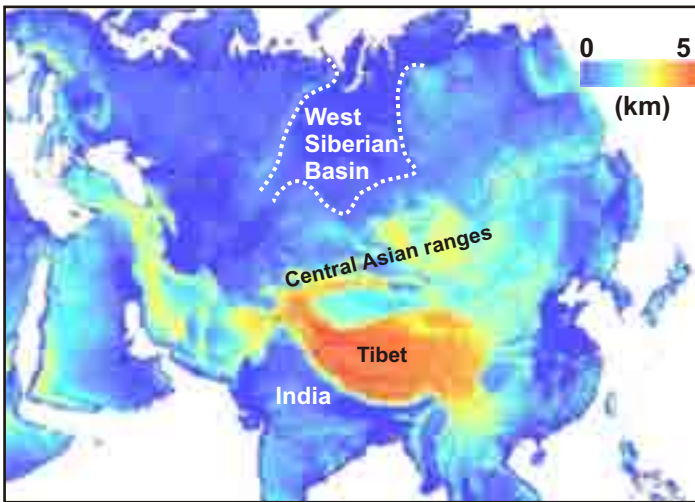


Figure 1

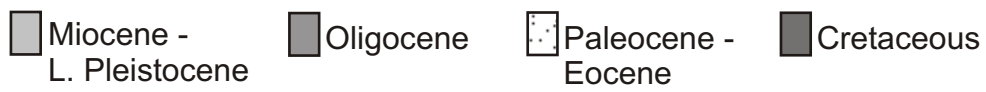
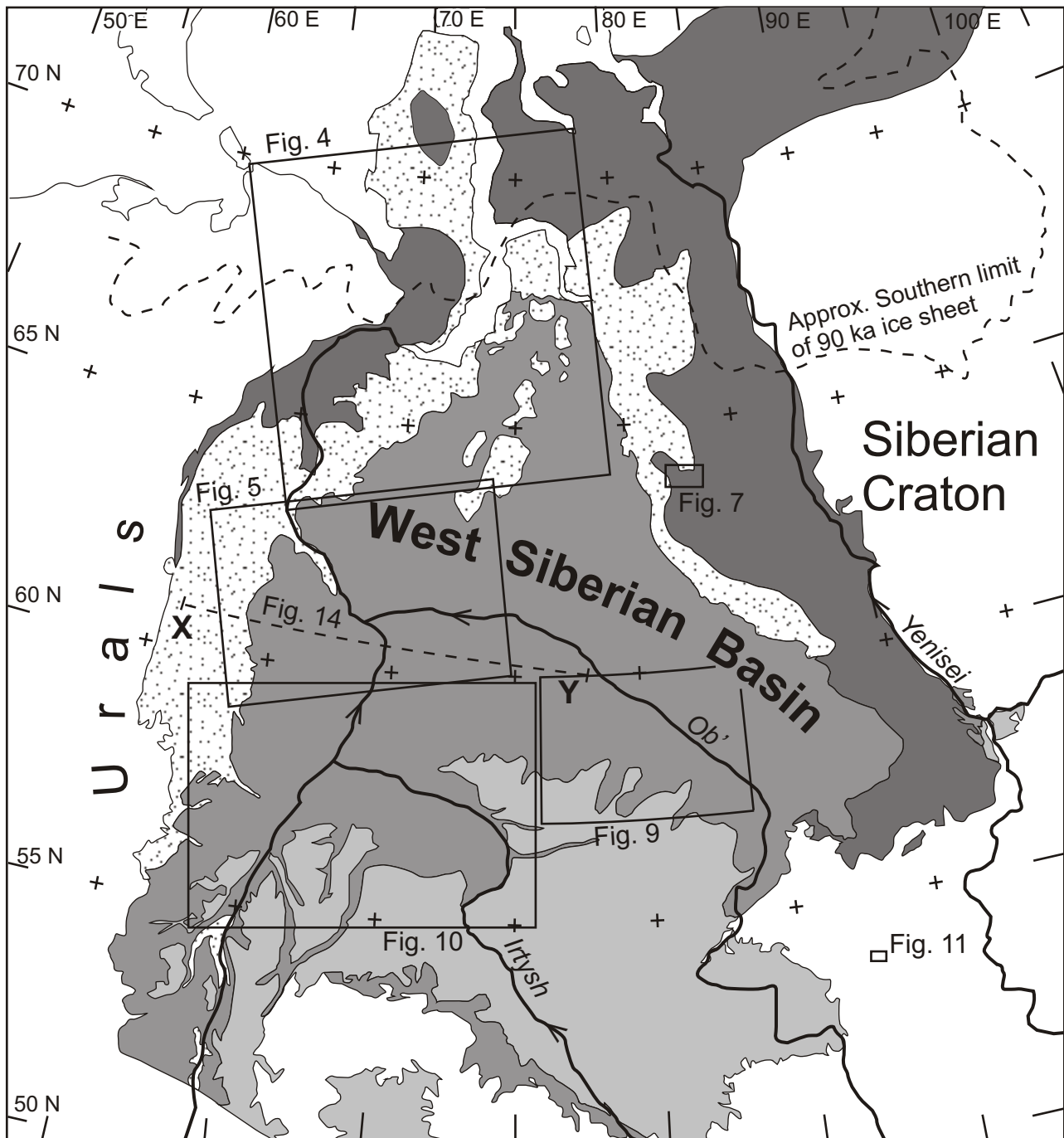


Figure 2

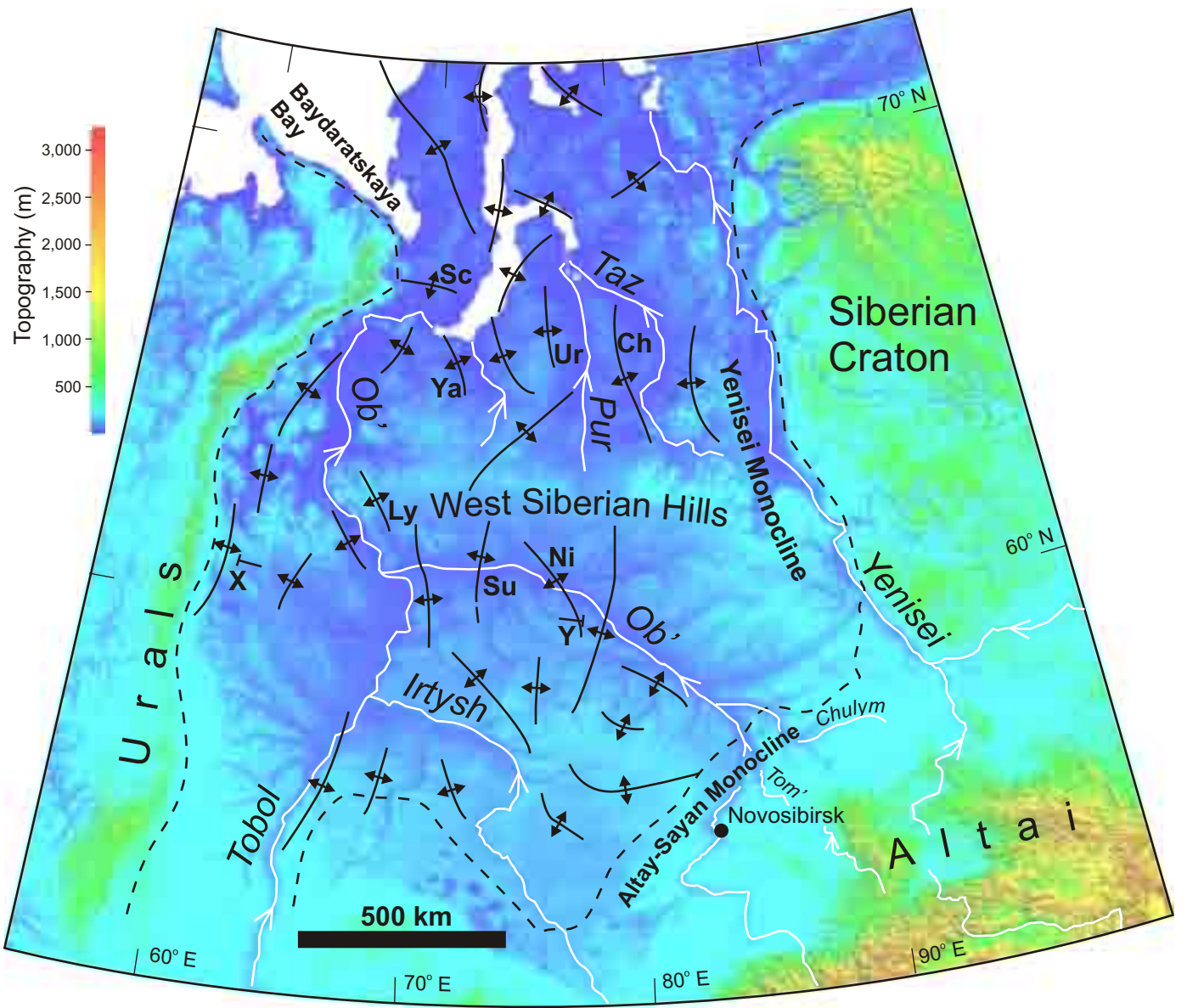


Figure 3

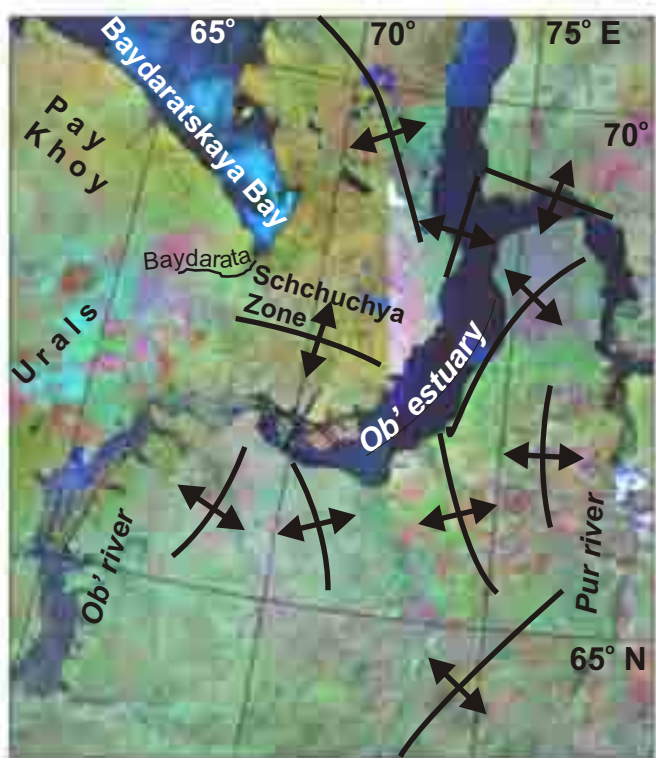


Figure 4

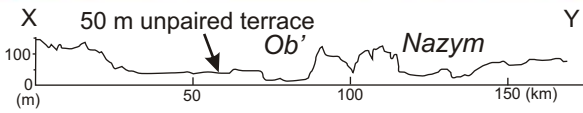
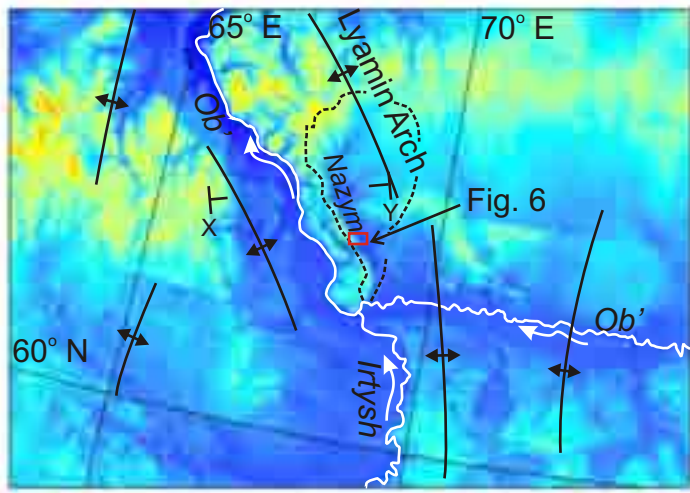


Figure 5

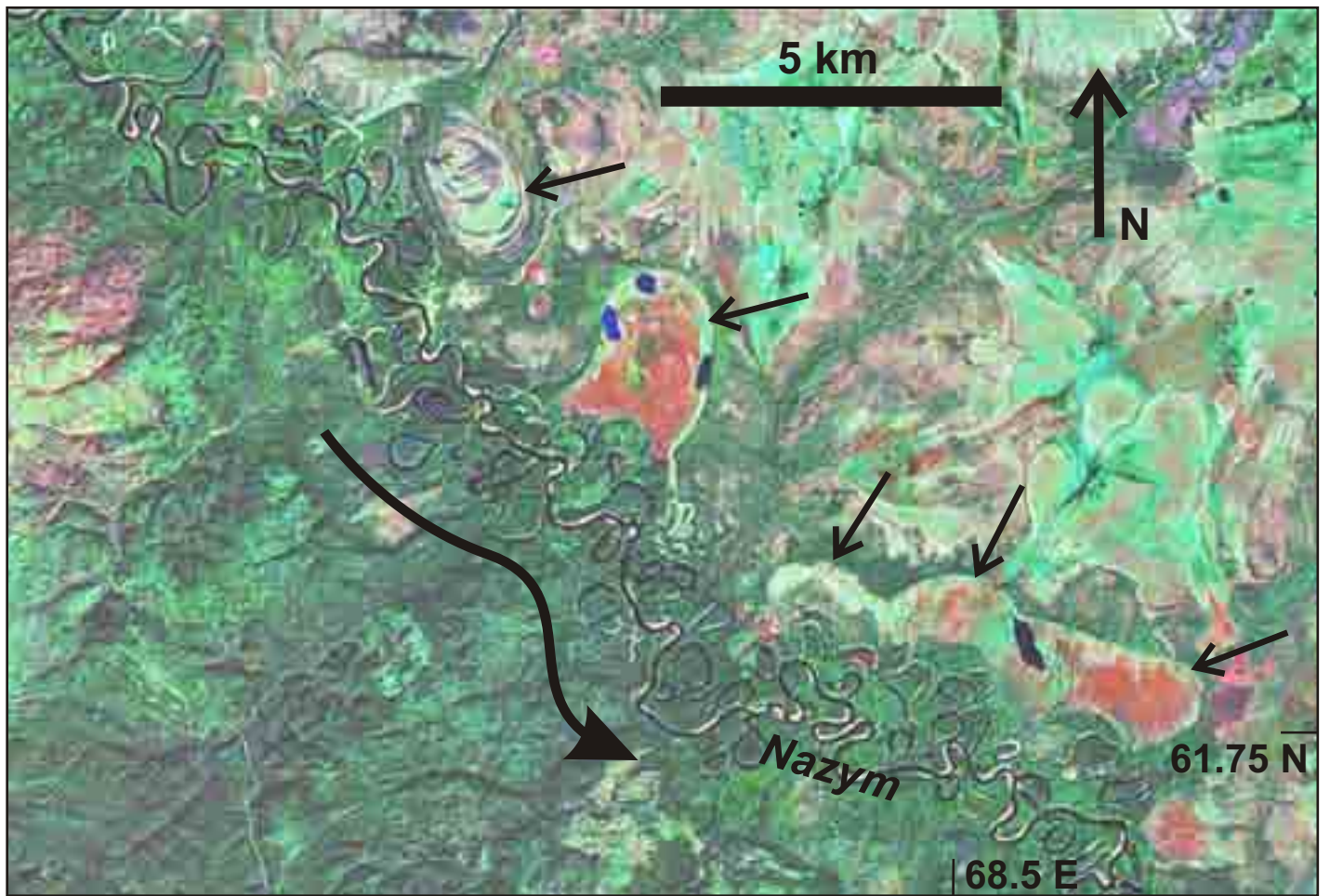


Figure 6

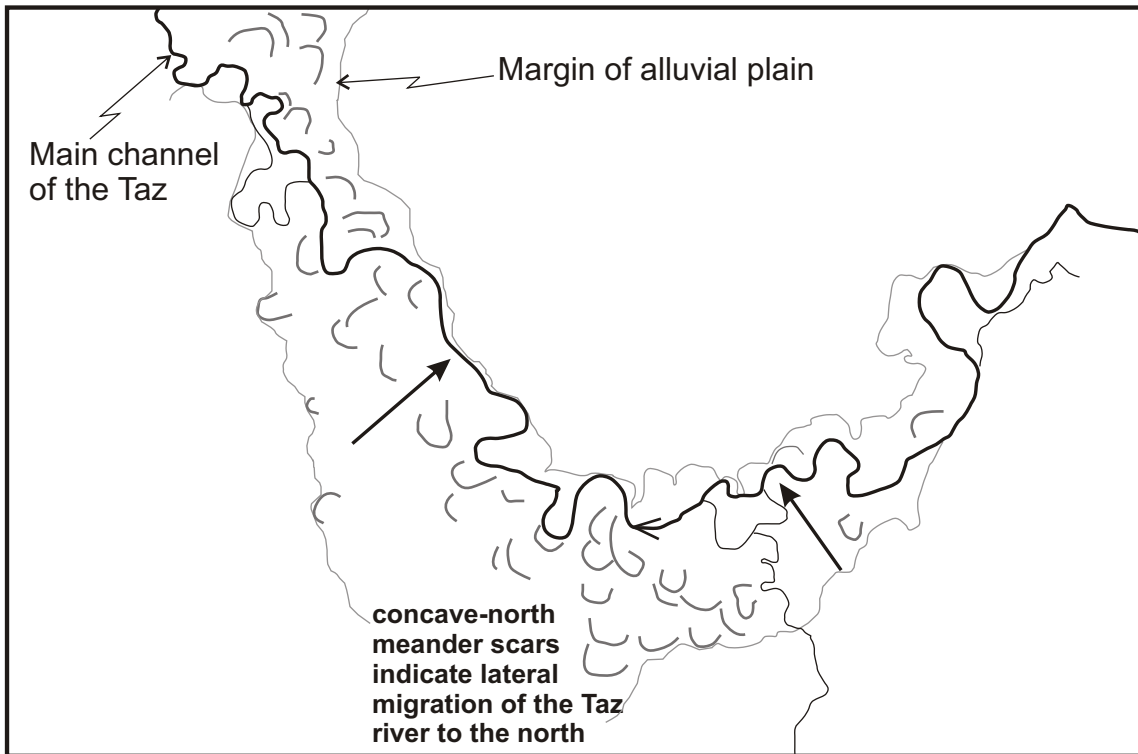
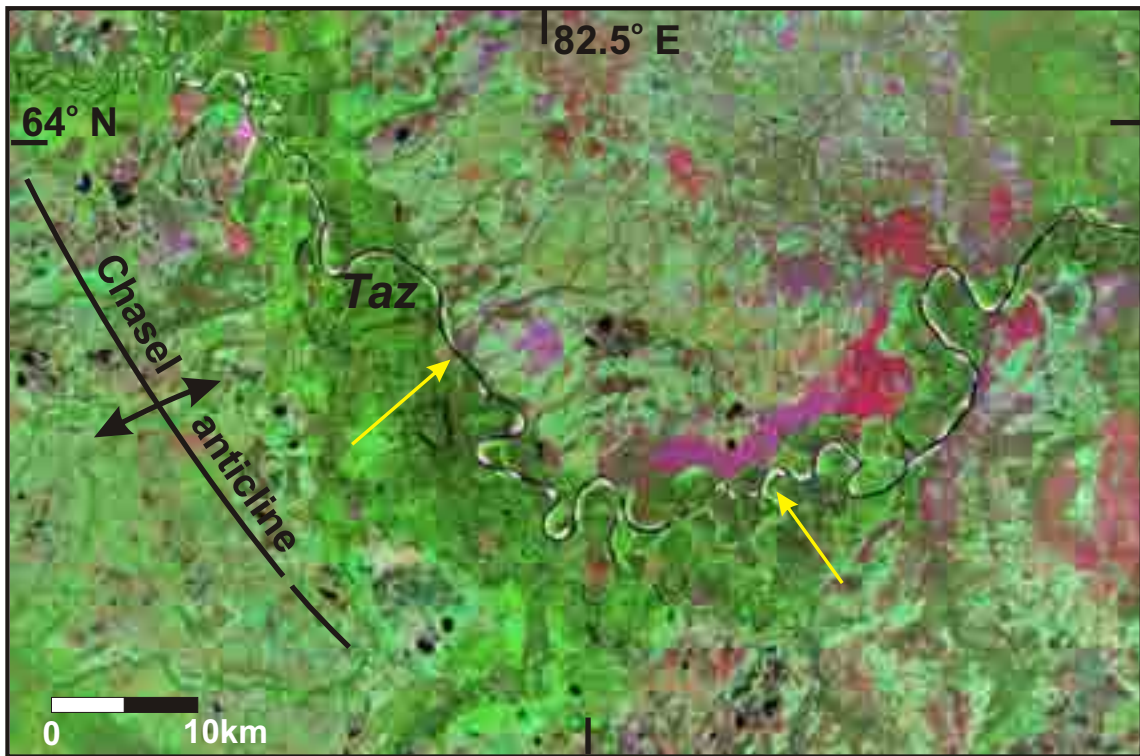


Figure 7

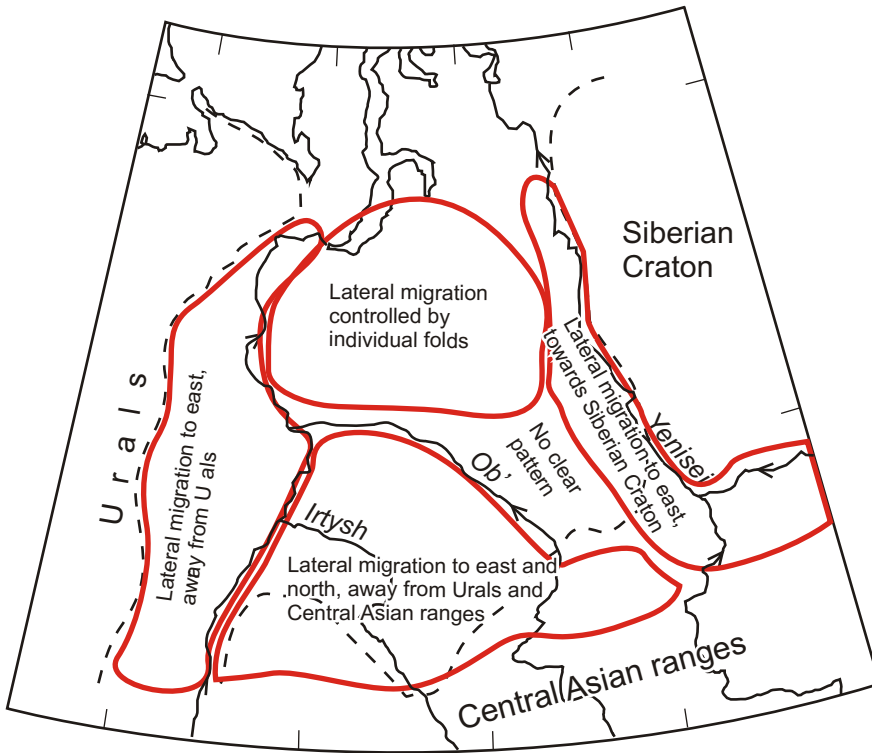
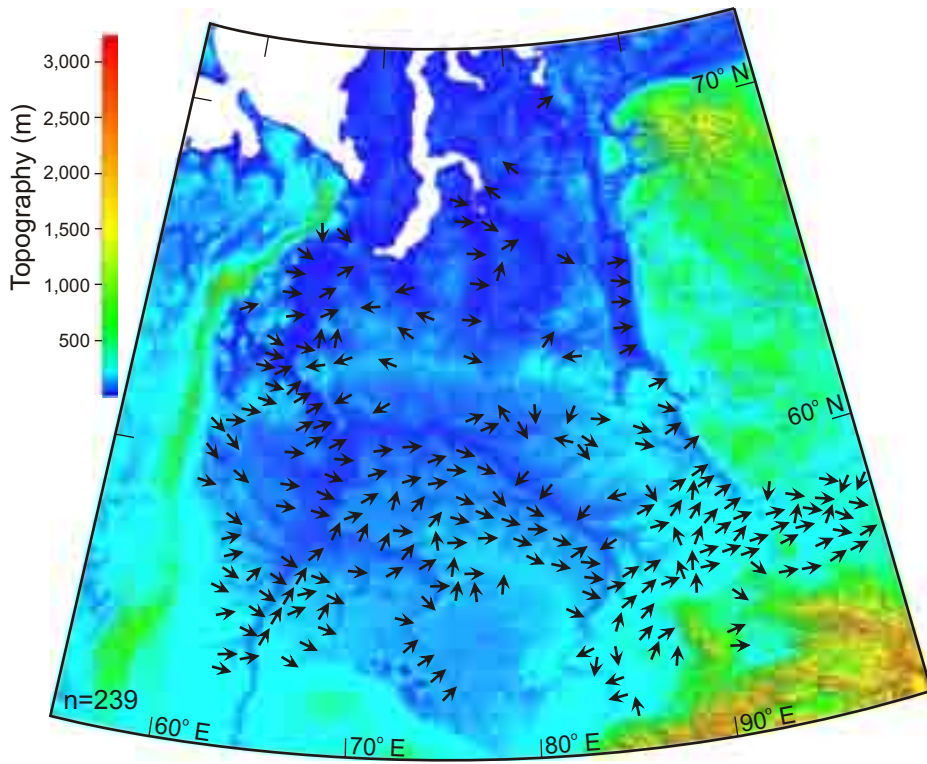


Figure 8

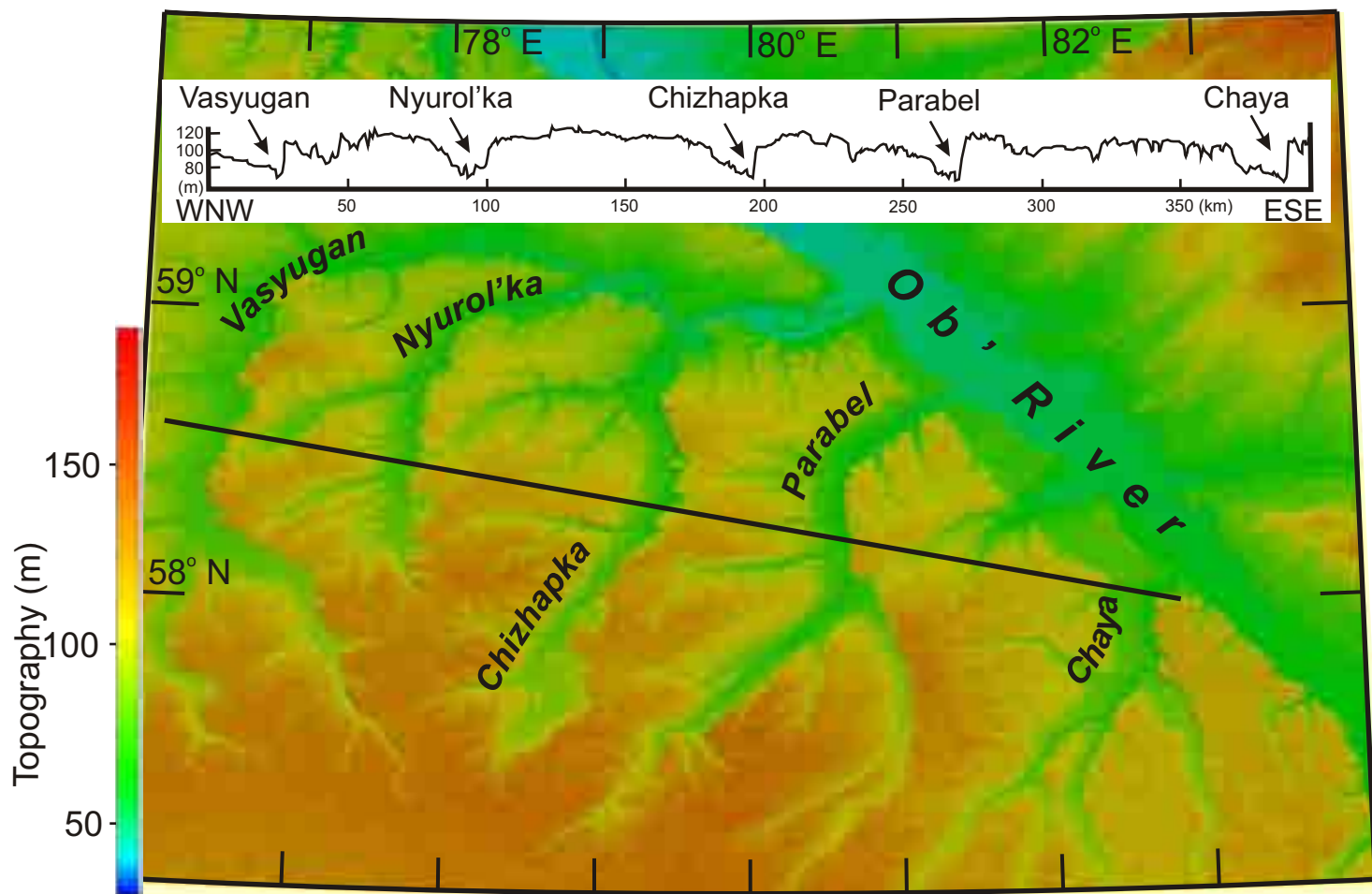


Figure 9

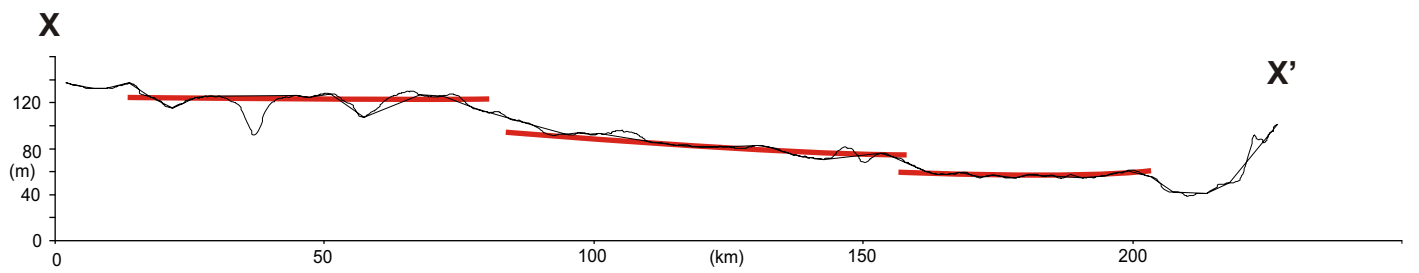
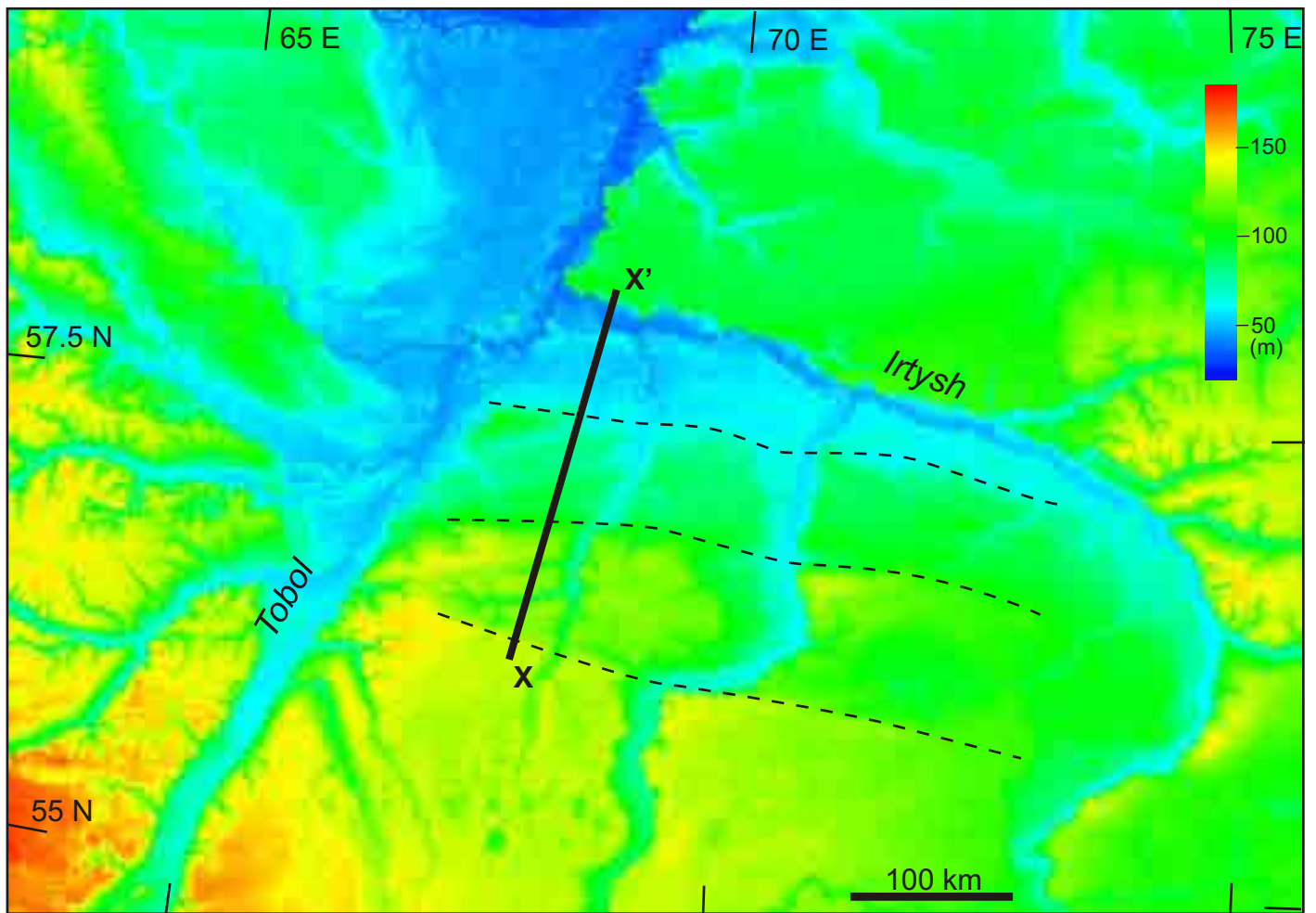


Figure 10

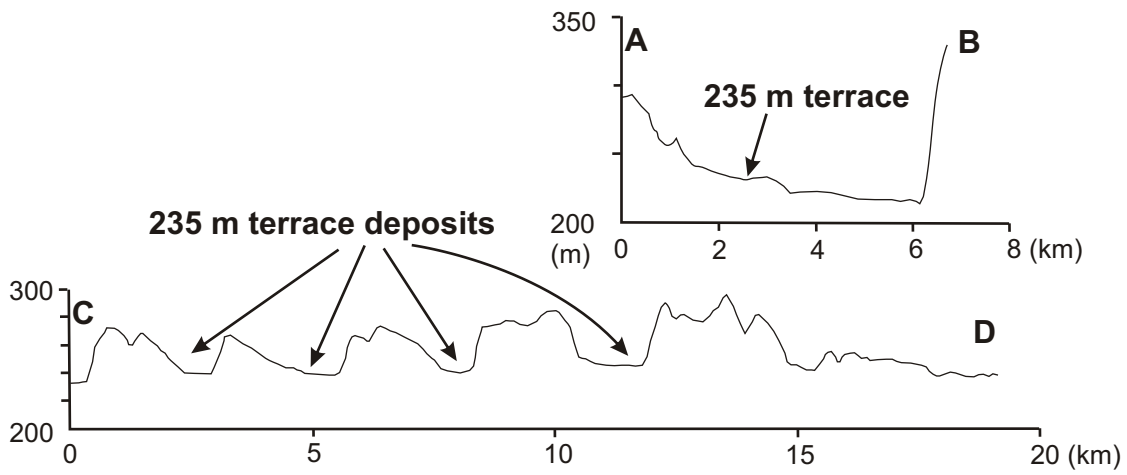
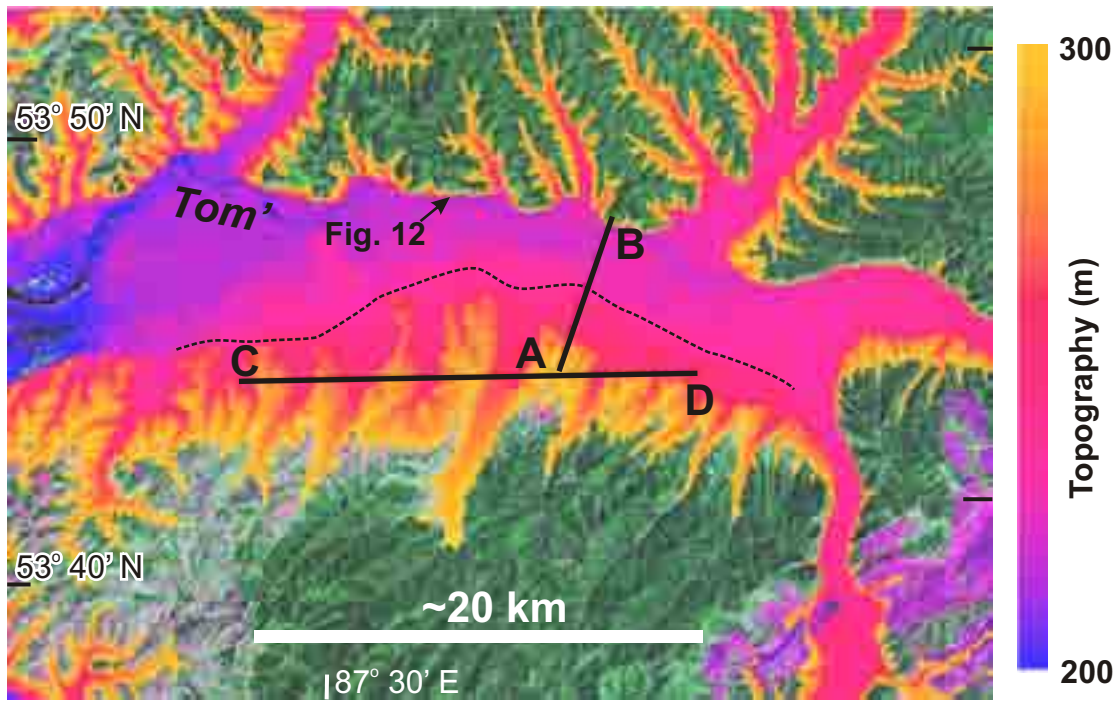


Figure 11



Figure 12



Figure 13

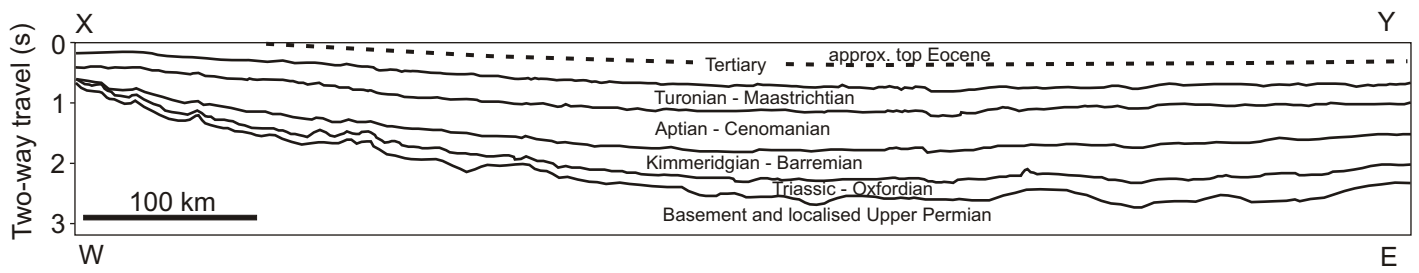


Figure 14